Süleyman Demirel Üniversitesi Fen Edebiyat Fakültesi Fen Dergisi
Süleyman Demirel University Faculty of Arts and Sciences Journal of Science
2021, 16(2): 533-543
DOI: 10.29233/sdufeffd.998966
Atıf için / For Citation: Y. A. Uncü, O. Karaman, H. Çakın, H. Özdoğan, "Calculation of mass attenuation coefficients for pedicle screw by theoretical and Monte Carlo simulation methods", *Süleyman Demirel Üniversitesi Fen Edebiyat Fakültesi Fen Dergisi*, 16(2), 533-543, 2021.

Research Article

Calculation of Mass Attenuation Coefficients for Pedicle Screw by Theoretical and Monte Carlo Simulation Methods

Yiğit Ali ÜNCÜ[1], Onur KARAMAN[2], Hakan ÇAKIN[3], Hasan ÖZDOĞAN[*4]

[1]*Akdeniz University, Vocational School of Technical Sciences, Department of Biomedical Equipment Technology, 07070, Antalya, Turkey*
[2]*Akdeniz University, Vocational School of Health Services, Department of Medical Imaging Techniques, 07070, Antalya, Turkey*
[3]*Akdeniz University, Faculty of Medicine, Department of Brain and Nerve Surgery, 07070, Antalya, Turkey*
[4]*Antalya Bilim University, Vocational School of Health Services, Department of Medical Imaging Techniques, 07190, Antalya, Turkey*

**corresponding author e-mail: hasan.ozdogan@antalya.edu.tr*

(Received: 23.09.2021, Accepted: 15.11.2021, Published: 25.11.2021))

Abstract: Spine fixation is required in cases such as congenital spinal curvatures, vertebral fractures, sagittal collapse over time, painful kyphosis, and bone load due to tumors. Although there are many methods in the literature, the most commonly used spine fixation method is the fixation with pedicle screws. In these cases, it is known that pedicle screws are used frequently in the body. In this study, how the radiological exposure of the pedicle screws in the vertebral column that dose was evaluated by simulation methods. First, the elemental analysis of the pedicle screw was analyzed via Scanning Electron Microscopy (SEM) equipped with the Energy Dispersive X-ray Spectroscopy (EDS). Then, the elemental compositions of the pedicle screw obtained were used for simulation codes. subsequently, the half-value thickness and the attenuation coefficient calculations were conducted for the pedicle screw and vertebral column. Both XCOM software and MCNP (Monte Carlo N-Particle) simulation code were used to obtain photon interaction parameters within the energy range of 60-250 keV.

Key words: Attenuation coefficient, MCNP, Pedicle screws, SEM, Vertebral column, XCOM

Pedikül Vidası İçin Kütle Zayıflama Katsayılarının Teorik ve Monte Carlo Simülasyon Teknikleri ile Hesaplanması

Öz: Konjenital omurga eğrilikleri, vertebra kırıkları, zamanla sagital kollaps, ağrılı kifoz, tümörlere bağlı kemik yükü gibi durumlarda omurga tespiti gerekir. Literatürde birçok yöntem olmasına rağmen en sık kullanılan omurga sabitleme yöntemi pedikül vidaları ile sabitlemedir. Bu durumlarda vücutta pedikül vidalarının sıklıkla kullanıldığı bilinmektedir. Bu çalışmada vertebral kolondaki pedikül vidalarının radyolojik maruziyetinin simülasyon yöntemleri ile nasıl değerlendirildiği araştırılmıştır. İlk olarak, pedikül vidasının element analizi, Enerji Dağıtıcı X-ışını Spektroskopisi (EDS) ile Taramalı Elektron Mikroskobu (SEM) ile analiz edildi. Daha sonra elde edilen pedikül vidasının elementel bileşimleri simülasyon kodları için kullanılmıştır. Daha sonra pedikül vidası ve vertebral kolon için yarı değer kalınlık ve zayıflatma katsayısı hesaplamaları yapılmıştır. Enerji aralığı 60-250 keV olan foton etkileşim parametrelerini elde etmek için hem XCOM yazılımı hem de MCNP (Monte Carlo N-Particle) simülasyon kodu kullanılmıştır.

Anahtar kelimeler: Zayıflatma katsayısı, MCNP, Pedikül vida, SEM, Vertebral kolon, XCOM

Yiğit Ali Üncü, yuncu@akdeniz.edu.tr, ORCID: https://orcid.org/0000-0001-7398-9540
Onur Karaman, onurkaraman@akdeniz.edu.tr, ORCID: https://orcid.org/0000-0003-3672-1865
Hakan Çakın, hcakın@akdeniz.edu.tr, ORCID: https://orcid.org/0000-0002-2635-4953
Hasan Özdoğan, hasan.ozdogan@antalya.edu.tr, ORCID: https://orcid.org/0000-0001-6127-9680

1. Introduction

The main principle in the surgical treatment as deformity, fracture, spondylolisthesis, tumor or disc degeneration is the stabilization and fusion of the pathological spine segment. The researcher described the first use of transpedicular screws after the other reported the use of screws aimed at fixing the facet joint in the spine [1-3].

The screw fixation of posterior transpedicular has become the method for instrumentation, especially in the lumbar and lumbosacral regions [4]. This technique is superior to other fixation methods used in the region, both biomechanical and clinical [4-6]. The pedicle screw is the center of force of the vertebra and all the forces applied through the pedicle are reflected on the vertebral body [7]. In this way, pedicle fixation provides control of the whole body and the stability provided by conventional methods. The idea that the correction effect and fusion rate will increase as the stability and power of the instrumentation increase, the use of pedicle screws has become widespread [8]. The successful prosthesis to replace damaged joints or bones was especially a cemented total hip prosthesis with a stainless steel stem developed [9].

Biocompatible metal alloys are frequently used in joint and bone implants due to their superior physical characteristics including mechanical strength, toughness, and ductility. Metallic biomaterials with resistance to corrosion and mechanical characteristics are used in the production of instruments as plates, screws, nails used for the fixation of the hip, knee, spine implants, and fractured structures. Stainless steels have been still in high demand as implant material in developing countries due to their relatively facilitate of manufacture, low cost, and reasonable resistance to corrosion [10]. Since the resistance to corrosion of Cobalt, Chromium alloys is better than that of stainless steel, Cobalt (Co), Nickel (Ni), Chromium (Cr), Molybdenum (Mo) alloys are used in stems of prosthetics of load-bearing joints such as hip and knee, and metal-metal hip implants [10-13]. It has been reported that elements as Co, Cr, Ni in stainless steel, and cobalt-chromium alloys are released into the body environment due to corrosion [14-16].

Titanium (Ti) alloys have excellent corrosion resistance to the inert Titanium Dioxide layer formed on the surface. Ti is one of the most used pedicle screws compounds which are widely used in the treatment of various physical disorders in the spine as orthopedic implants. Aluminum (Al) and vanadium (V) alloying elements improve the mechanical properties and microstructure [10]. These alloying elements are considered to be safer compared to V and Al, and alloys have advantages such as elastic modulus close to that of human bone, excellent corrosion resistance, and high specific strength [17-19].

Radiation attenuation occurring in the tissues between the relevant biological materials and the detector is one of the most crucial issues in the use of γ-rays in radiology. For this reason, measurements of the half-value thickness (layer) of biological materials are important linear attenuation coefficients and related mass attenuation coefficients, which are defined as the probability of photon interaction with a particular material per unit path length for crucial in radiation-related issues.

The radiological methods depend on the transmission, absorption, or scattering of the radiation beam from body organs and tissues in body structures [20]. Problems in applying unacceptably high radiation doses to patients in radiological methods can be minimized by a good estimate of the thickness of the biological materials in the radiation path and careful selection of the radiation source-related radiology. Accurate data on these quantities for narrow beam geometries are essential for γ-rays in areas such as radiology imaging, nuclear medicine, radiotherapy. Measurements of half-value

layer and attenuation coefficients using many techniques and materials have been made by different groups [20-26].

Recently, the important program that makes nuclear interactions using the Monte Carlo (MC) Simulation Code has taken its place as MCNP (Monte Carlo N-Particle). The Energy Dispersive X-ray Spectroscopy is the most effective Scanning Electron Microscopy (SEM) attachment Dispersive X-ray Spectroscopy (EDS). The EDS system can provide atomic, qualitative, and quantitative data from the specimen. The EDS results which are characteristic of the pedicle screw's atomic structure to be distinguished from one another have been used by computer-aided simulation and calculation codes with XCOM and MCNP6. Obtained results via both codes have been compared and these results have been graphed for better visual understanding.

2. Material and Method

In the present study, the SEM-EDS analysis of pedicle screw has been conducted to obtain an elemental composition whose knowledge is crucial for MC simulations. The half-value layer and mass attenuation coefficients of the pedicle screw and vertebral column have been calculated by using MCNP6 software. Obtained results have been compared the National Institute of Standards and Technology database via XCOM.

2.1 Scanning electron microscopy analysis

SEM is a tool that creates magnified images that reveal information on a microscopic scale about the size, shape, composition, crystallography, and other physical and chemical properties of a sample [27]. The basic working principle of SEM is the image formation by processing the data obtained as a result of the interaction of electrons released from the electron source with the sample by the sensors. The image is formed by the signals that occur as a result of the interaction of the sample surface under investigation with the electron beam [28]. SEM is a technique used to image the surface of a sample, and three-dimensional images can be obtained with this technique.

2.2 Energy dispersive x-ray spectroscopy

The EDS system can provide atomic, qualitative, and quantitative data from the sample. It focuses on the study of X-rays produced by matter in place of the impact of charged particles and examines a sample through the interactions between electromagnetic radiation and material. Their characterization abilities are largely due to the basic concept that each element has an atomic structure and distinguishes X-rays, which are characteristic of an element's atomic structure [25-28].

In this study, to lighten up the surface morphology and elemental composition of the pedicle screw SEM ZEISS Gemini SEM equipped with EDS- QUANTAX was used. The microscope obtained the conditions such as voltage 20 kV, current as 8-10 nA, the beam diameter of 100 μm, decreased vacuum in the chamber with the pressure of 50 Pa.

2.3 Attenuation parameters

The γ-ray or X-ray radiations, the intensity of the beam are attenuated for the Beer-Lambert's law [23] equation as follow,

$$I = I_0 e^{-\mu x} \tag{1}$$

The μ (cm^{-1}) is the linear attenuation coefficient for a material, where I is the attenuated photon intensity and I_o is unattenuated photon intensity, x (cm) is the thickness. A coefficient is characterizing a given material is the density-independent, mass

attenuation coefficient. The rearrangement of Equation 1 obtained to the equation for the linear attenuation coefficient [24];

$$\mu = \frac{1}{x} ln(I_0/I) \quad (2)$$

The mass attenuation coefficients for the materials were obtained from Equation 2 with the density of corresponding samples as;

$$\mu/\rho = \frac{1}{\rho x} ln(I_0/I) \quad (3)$$

The mass attenuation $\mu/\rho(cm^2g^{-1})$, where ρ (gcm^{-3}) is the measured density of the material, and I is the attenuated photon intensity and Io unattenuated photon intensity and x (cm) is the thickness in Equation 3 and obtained from Equation 2. for half-value layer (cm), is the thickness of material for which the intensity in Equation 4 [24, 26].

$$x_{1/2} = \frac{ln\,2}{\mu} \quad (4)$$

2.4 Simulations

The XCOM software is possible to obtain photon cross-section data for a single element, compound, or mixture. It was used to calculate theoretical values of the half-value layer and mass attenuation coefficients (μm) of the samples for γ-rays at photon energies of 60 –250 keV [36]. In nuclear physics, numerous computer codes, based on analytical approximations [30-36] and MC techniques [37-43], are widely used by researchers. MC techniques can be used in the solution of probabilistic processes such as radiation transport as well as in a complex integral calculation that is not practical to solve [44]. MC techniques are statistical methods used to study arbitrary behaviors that cannot be handled analytically on a computer. Most of the calculations are based on repeatable, arbitrary numbers that are uniformly distributed, providing a variety of statistical tests, and produced in the range (0,1). Since these numbers are not uniformly distributed and independent from each other, these numbers produced by the computer are called so-called random numbers. Nuclear libraries embedded in code systems contain the possibilities of interaction of each atom at each energy [45]. The random numbers produced by MC codes are used to decide which event will occur over these probability distributions.

The distribution of random numbers used in calculations made by the MC method affects the result. The random numbers generated must be regular random numbers. Calculations using probabilistic random numbers stacked in one section bring errors [46]. In our study, all calculations have been carried out by employing two of the best known and frequently used computer-aided simulation and calculation tools which are XCOM and MCNP6 [47]. The half-value layer and mass attenuation coefficients of the pedicle screw and the vertebral column have been calculated. The MCNP6 geometry can be seen in Figure 1. In MCNP simulations 5×10^6 photons were used as a number of particles with computer hardware(Intel Core I7 CPU 2.6 GHz).

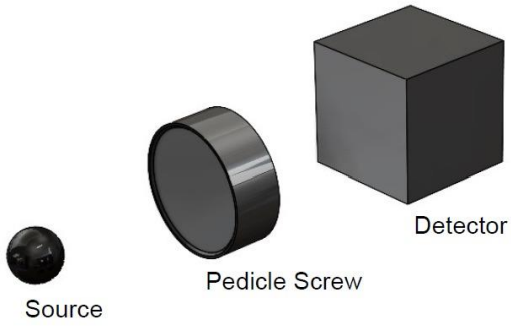

Figure 1. MCNP Geometry used in simulations

3. Results

The surface morphology and elemental composition of the pedicle screw have been obtained from scanning SEM-EDS. As depicted in Figure 2(a), the smooth and homogenous morphology has been detected for the bottom side of the pedicle screw in Figure 2(a) and related EDS analysis of the pedicle screw in Figure 2(b).

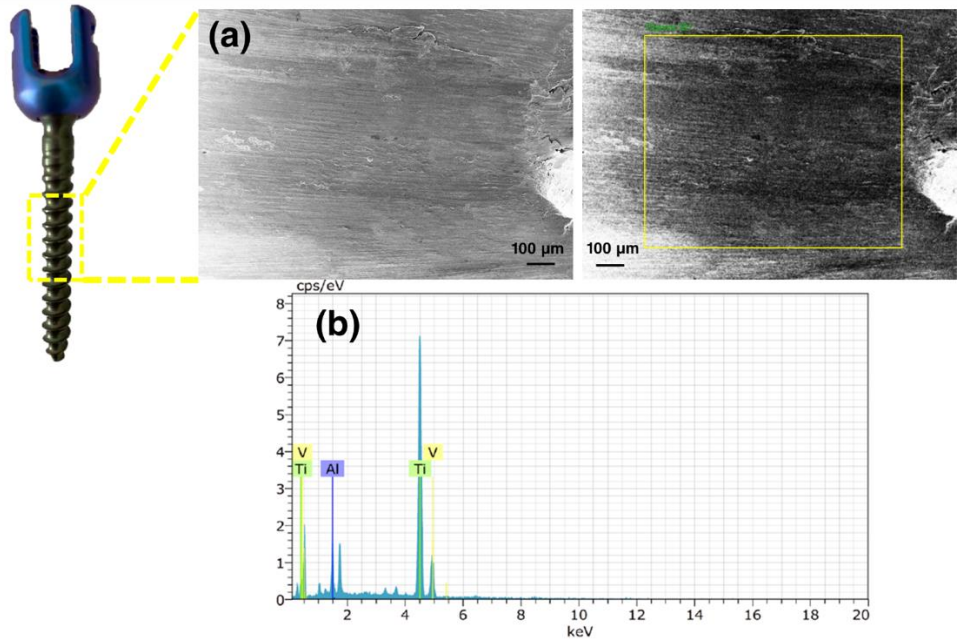

Figure 2. (a) SEM images (**b)** related EDS analysis of pedicle screw

The SEM-EDS analysis of the related region (yellow-lined in Figure 2(a)) has been demonstrated that the pedicle screw has been composed of Ti (89.11%), Al (8.54%), and V (2.35%) (Table 1).

Table 1. % Elemental composition of pedicle screw

Ti	**Al**	**V**
89.11	8.54	2.35

The mass attenuation coefficients of the pedicle screw were calculated by using the elemental composition which is obtained from SEM-EDS analysis as seen in Figure 2 and elemental composition values in Table 1. In addition to pedicle screw calculations, the mass attenuation coefficients of the vertebral column were calculated. Elemental compositions of the vertebral column, which have been shown in Table 2, are obtained from the literature [48].

Table 2. %Elemental composition of vertebral column [48]

H	C	N	O	Na	Mg	P	S	Cl	K	Ca	Fe
7.098	25.792	3.599	47.186	0.1	0.1	5.098	0.3	0.1	0.1	10.497	0.03

Photon interaction parameters of the pedicle screw and vertebral column were calculated for radiological energies. The density of pedicle screw is $\rho = 4.56\ g\ cm^{-3}$ and vertebral column is $\rho = 1.33\ g\ cm^{-3}$ [48]. The mass attenuation coefficients values of the pedicle screw and vertebral column were calculated using Equation 3. The half-value layer of the pedicle screw and vertebral column were calculated using Equation 4. The half-value layer and mass attenuation coefficients of results have been presented in Table 3. Especially at low photon energy mass attenuation coefficients of the pedicle screw were found to be much higher than the vertebral column. The mass attenuation coefficients of the pedicle screw approximately are three times that of the vertebral column at 60 keV. This huge difference is a problem for radiological imaging. In addition to mass attenuation coefficients, half-value layers were calculated by using MCNP6 results.

Table 3. Calculated values of mass attenuation coefficients (cm^2g^{-1}) and half-value layer (cm) for pedicle screw and vertebral column

Energy (keV)	Pedicle screw (MCNP)	Pedicle screw (XCOM)	Vertebral Column (MCNP)	Vertebral Column (XCOM)	Differences (μ/ρ)Vertebral Column - Pedicle screw	HVL (Pedicle Screw)	HVL (Vertebral Column)
60	0.72610	0.72620	0.25480	0.2548	-0.4713	0.20934577	2.04538184
70	0.45259	0.51110	0.22076	0.2213	-0.23183	0.33585797	2.36076868
80	0.38841	0.38860	0.20106	0.2007	-0.18735	0.3913544	2.59207845
90	0.28605	0.31310	0.18764	0.1868	-0.09841	0.53139647	2.77746373
100	0.26436	0.26380	0.17734	0.1766	-0.08702	0.57499607	2.93878027
110	0.21592	0.22980	0.16929	0.1688	-0.04663	0.70399204	3.0785238
120	0.19497	0.20550	0.16348	0.1625	-0.03149	0.77963769	3.18793304
130	0.17945	0.18740	0.15811	0.1572	-0.02134	0.84706582	3.29620703
140	0.16749	0.17360	0.15319	0.1526	-0.0143	0.90755245	3.40207124
150	0.16315	0.16260	0.14961	0.1486	-0.01354	0.93169452	3.483479
160	0.15041	0.15380	0.14603	0.145	-0.00438	1.01061073	3.56887827
170	0.14372	0.14650	0.14290	0.1418	-0.00082	1.0576535	3.64704894
180	0.13768	0.14040	0.13977	0.1388	0.00209	1.10405259	3.72872071
190	0.13322	0.13520	0.13709	0.136	0.00387	1.14101457	3.80161422
200	0.13099	0.13060	0.13441	0.1335	0.00342	1.16043943	3.87741458
210	0.12549	0.12660	0.13217	0.1311	0.00668	1.21129939	3.9431285
220	0.12221	0.12310	0.12994	0.1289	0.00773	1.24380951	4.01079955
230	0.11920	0.12000	0.12770	0.1268	0.0085	1.27521779	4.08115344
240	0.11671	0.11710	0.12547	0.1248	0.00876	1.30242448	4.15368848

250	0.11422	0.11450	0.12368	0.1229	0.00946	1.33081738	4.21380412

For visualizationMCNP6 and XCOM results have been presented for pedicle screw and vertebral column in Figure 3-4 respectively. MCNP6 results have consisted of XCOM data for both elements.

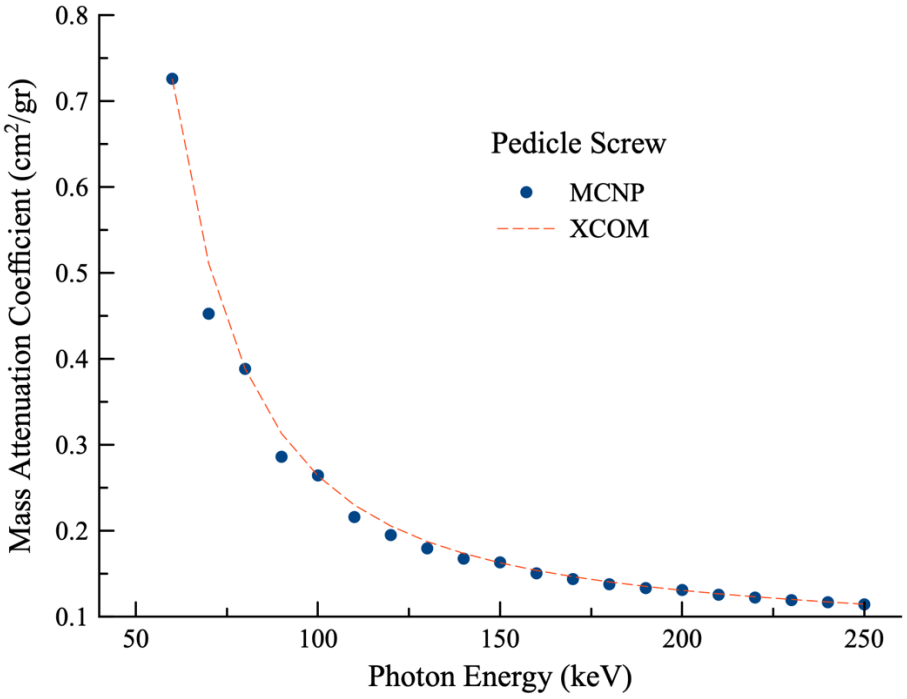

Figure 3. Comparison of the calculated mass attenuation coefficients for pedicle screw via XCOM and MCNP

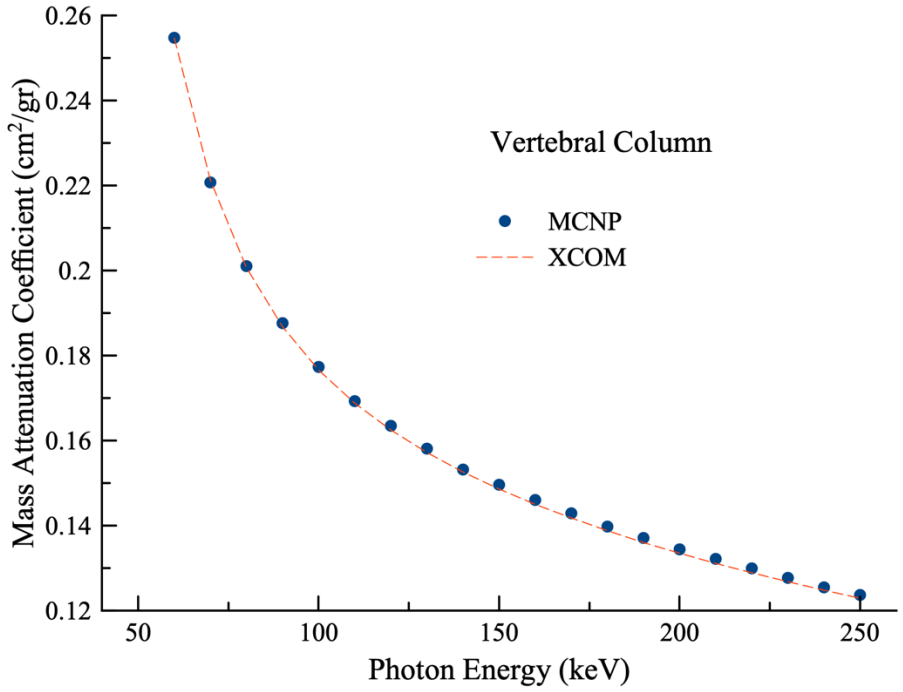

Figure 4. Comparison of the calculated mass attenuation coefficients for vertebral column via XCOM and MCNP

4. Conclusion and Comment

Pedicle screws are widely used in the treatment of various physical disorders in the spine. Vertebral transpedicular screws are routinely used in the treatment of degenerative or traumatic abnormalities of the vertebra. The density and model in which pedicle screws are used differ widely in clinical practice to support, the weight of the torso and are often used in the lumbar vertebra, the largest in the vertebral column. Therefore, it is very important that the fixation of pedicle screws to the vertebrae absorb the dose in routine radiologic examinations.

Studies on this subject have led to improvements in the screw placement technology and the design of screws and plates. Recently, there are various studies on screw implantation, proper screw selection, and screw strength. Although the importance of radiological investigation of the location of the pedicle screw on the spine is emphasized, the lack of the half-value layer and mass attenuation coefficients of the pedicle screw calculations are among the main shortcomings.

The elemental analysis of the pedicle screw sample was made by SEM-EDS in Figure 2(b) and elemental analysis (Table 1) results were used in MCNP and XCOM. Photon interaction parameters of the pedicle screw and vertebral column (Table 2) were calculated with MCNP6 for radiological energies (60 keV-250 keV) and compared with XCOM data (Table 3). It is seen; the mass attenuation coefficient results obtained by MCNP6 simulation and XCOM data in Figure 3-4. This fit is important for the validation of the MCNP6 results, and the result is supported by the result that the MC method is a powerful and flexible tool in such studies. As it is demonstrated that the mass attenuation coefficients of the pedicle screw and vertebral column are different. Differences are too high at radiological imaging energies. This study focused on finding the difference between mass attenuation coefficients of the pedicle screw and vertebral column. This difference may cause artifacts during radiological imaging.

Author Statement

Yiğit Ali Üncü: Conceptualization, Investigation, Review and Editing, Original Draft Writing.
Onur Karaman: Visualization, Formal Analysis, Resource/Material/Instrument Supply.
Hakan Çakın: Conceptualization, Validation, Investigation, Data Curation.
Hasan Özdoağan: Methodology, Software, Supervision, Observation, Advice, Project Administration.

Acknowledgment

The authors very much appreciate the support to the density value of pedicle screw by Kayahan Medical, Turkey for providing Orion brand pedicle screw.

Conflict of Interest

As the authors of this study, we declare that we do not have any conflict of interest statement.

Ethics Committee Approval and Informed Consent

As the authors of this study, we declare that we do not have any ethics committee approval and/or informed consent statement.

References

[1] R. Skinner, J. Maybee, E. Transfeldt, R. Venter, W. Chalmers, "Experimental pullout testing and comparison of variables in transpedicular screw fixation. A biomechanical study," *Spine.*, 15, 195-201, 1990.
[2] H. H. Boucher, "A method of spinal fusion," *J. Bone Jt. Surg.*, 41, 248-259, 1959.
[3] B. S. Myers, Jr.P.J. Belmont, W. J. Richardson, R. Y. James, K. D. Harper, and R. W. Nightingale, "The role of imaging and in situ biomechanical testing in assessing pedicle screw pull-out strength," *Spine.*, 21, 1962-1968, 1996.
[4] N. A. Ebraheim, R. Xu, M. Darwich, and R. A. Yeasting, "Anatomic relations between the lumbar pedicle and the adjacent neural structures," *Spine.*, 22, 2338-2341, 1997.
[5] R. B. Ashman, R. D. Galpin, J. D. Corin, and C. E. Johnston, "2d. Biomechanical analysis of pedicle screw instrumentation systems in a corpectomy model," *Spine.*, 14, 1398-405, 1989.
[6] M. H. Krag, B. D. Beynnon, M. H. Pope, and T. A. DeCoster, "Depth of insertion of transpedicular vertebral screws into human vertebrae: effect upon screw-vertebra interface strength," *Clin. Spine Surg.*, 1, 287-294, 1989.
[7] A. D. Steffee, R. S. Biscup, and D. J. Sitkowski, "Segmental spine plates with pedicle screw fixation. A new internal fixation device for disorders of the lumbar and thoracolumbar spine," *Clin. Orthop. Relat. Res.*, 203, 45-53, 1986.
[8] G. Lynn, D. P. Mukherjee, R. N. Kruse, K. K. Sadasivan, and J. A. Albright, "Mechanical stability of thoracolumbar pedicle screw fixation. The effect of crosslinks," *Spine.*, 22, 1568-73, 1997.
[9] J. Charnley, "Anchorage of the femoral head prosthesis to the shaft of the femur," *J. Bone Jt. Surg.*, 42, 28-30, 1960.
[10] F. Mahyudin, L. Widhiyanto, and H. Hermawan, "Biomaterials in orthopaedics.," Ed. Mahyudin F, Hermawan H. Biomaterials and Medical Devices A Perspective from an Emerging Country, Cambridge, UK, Springer. 2016, pp. 161-181.
[11] F. Á. Rodríguez-González, "Introduction to biomaterials in orthopaedic surgery," Ed. Rodriguez-Gonzalez FÁ, Biomaterials in Orthopaedic Surgery. Ohio, USA, ASM International. 2009, pp. 1-10.
[12] B. Patel, G. Favaro, F. Inam, M. J. Reece, A. Angadji, W. Bonfield, W. J. Huang, and M. Edirisinghe, "Cobalt-based orthopaedic alloys: Relationship between forming route, microstructure and tribological performance," *Mater. Sci. Eng. C.*, 32, 1222-1229, 2012.
[13] C. Zhao, J. Zhou, Q. Mei, and F. Ren, "Microstructure and dry sliding wear behavior of ultrafine-grained Co-30 at% Cr alloy at room and elevated temperatures," *J. Alloys Compd.*, 770, 276-284, 2019.
[14] Y. Okazaki, E. Gotoh, "Comparison of metal release from various metallic biomaterials in vitro," Biomaterials., 26(1), 11-21, 2005.
[15] K. L. Wapner, "Implications of metallic corrosion in total knee arthroplasty," *Clin. Orthop. Relat. Res.*, 271, 12-20, 1991.
[16] D. B. McGregor, R. A. Baan, C. Partensky, J. M. Rice, and J. D. Wilbourn, "Evaluation of the carcinogenic risks to humans associated with surgical implants and other foreign bodies - A report of an IARC Monographs Programme," *Meeting. Eur. J. Cancer*, 36, 307-313, 2000.
[17] S. Bahl, S. Das, S. Suwas, and S. K. Chatterjee, "Engineering the next-generation tin containing β titanium alloys with high strength and low modulus for orthopedic applications," *J. Mech. Behav. Biomed. Mater.*, 78, 124-133, 2018.
[18] M. Niinomi, M. Nakai, and J. Hieda, "Development of new metallic alloys for biomedical applications,"*Acta. Biomater.*, 8, 3888-3903, 2012.
[19] R. Zhou, D. Wei, J. Cao, W. Feng, S. Cheng, Q. Du, B. Li, Y. Wang, D. Jia, and Y. Zhou, "Metallic implant biomaterials," *ACS Appl. Mater. Interfaces. 7*, 8932-8941, 2015.
[20] O. Kovalchuk, A. Ponton, J. Filkowski, and I. Kovalchuk, "Dissimilar genome response to acute and chronic low-dose radiation in male and female mice," *Mutat. Res-Fund Mol. M.*, 550, 59-72, 2004.
[21] C. M. Davisson and R. D. Evans, "Gamma-ray absorption coefficients," *Rev. Mod. Phys.*, 24, 79, 1952.
[22] D. M. Taylor, "The radiopharmaceutical and its interaction with the patient," In: Mores BM, Parker RP, Pullan BR, Ed. Physicalaspect medical imaging. New York: Wiley, 1981.
[23] I.I. Bashter, "Calculation of radiation attenuation coefficients for shielding concretes," *Ann. Nucl. Energy*, 24, 1389-1401, 1997.
[24] M. A. Abdel-Rahman, E. A. Badawi, Y. L. Abdel-Hady, and N. Kamel, "Effect of sample thickness on the measured mass attenuation coefficients of some compounds and elements for 59.54, 661.6 and 1332:5 keV g-rays," *Nucl. Instrum. Methods Phys. Res. A: Accelerators, Spectrometers, Detectors and Associated Equipment*, 447, 432-436, 2000.
[25] K. Singh, G. Kaur, G. K. Sandhu, and B. S Lark, "Interaction of photons with some solutions," *Radiat. Phys. Chem.*, 61, 537-540, 2001.

[26] B.Z. Shakhreet, C.S. Chong, T. Bandyopadhyay, D.A. Bradley, A.A. Tajuddin, A. Shukri, "Measurement of photon mass-energy absorption coefficients of paraffin wax and gypsum at 662 keV," *Radiat. Phys. Chem.*, 68, 757-764, 2003.
[27] J. E. Rossen and K. L. Scrivener, "Optimization of SEM-EDS to determine the C–A–S–H composition in matured cement paste samples," *Mater. Charact.*, 123, 294-306, 2017.
[28] K. Rokosz, T. Hryniewicz, S. Raaen, P. Chapon, and Ł. Dudek, "GDOES, XPS, and SEM with EDS analysis of porous coatings obtained on titanium after plasma electrolytic oxidation," *Surf. Interface Anal.*, 49, 303-315, 2017.
[29] H. Yücel, E. Güllüoglu, S. Çubukçu, Y. A Üncü, "Measurement of the attenuation properties of the protective materials used as a thyroid guard and apron for personnel protection against diagnostic medical x-rays," *J. Phys. Sci.*, 27, 111, 2016.
[30] S. Y. Darki and S. Keshavarz, "Studies on mass attenuation coefficients for some body tissues with different medical sources and their validation using Monte Carlo codes," *Nucl. Sci. Tech.*, 31(12), 1-15, 2020.
[31] H. Özdoğan, "Theoretical calculations of production cross–sections for the 201Pb, 111In 18F and 11C radioisotopes at proton induced reactions," *Appl. Radiat Isot*., 143, 1-5, 2019.
[32] M. Şekerci, H. Özdoğan, and A. Kaplan, "Investigation on the different production routes of 67Ga radioisotope by using different level density models," *Mosc. Univ. Phys. Bull.*, 74, 277-281, 2019.
[33] M. Şekerci, H. Özdoğan, and A. Kaplan, "An investigation of effects of level density models and gamma ray strength functions on cross-section calculations for the production of 90Y, 153Sm, 169Er, 177Lu and 186Re therapeutic radioisotopes via (n,γ) reactions.," *Radiochim. Acta*., 108, 11-17, 2020.
[34] H. Özdoğan, M. Şekerci, and A. Kaplan, "A new developed semi empirical formula for the α p reaction cross section at 19 1 MeV," *Mod. Phys. Lett. A*, 34, 1950044, 2019.
[35] A. Kaplan, M. Şekerci, V. Çapalı, and H. Özdoğan, "Photon induced reaction cross section calculations of several structural fusion materials," *J. Fusion Energy*, 36, 213-217, 2017.
[36] A. Kaplan, M. Şekerci, H. Özdoğan, and B. Demir, "A study on the calculations of cross–sections for 66,67gA and 75sE radionuclides production reactions via 3He particles," *Eskişehir Technical University Journal of Science and Technology A-Applied Sciences and Engineering*, 21, 554-56, 2020.
[37] H. Özdoğan, M. Şekerci, and A. Kaplan, "Investigation of gamma strength functions and level density models effects on photon induced reaction cross section calculations for the fusion structural materials 46 50Ti 51V 58Ni and 63Cu," *Appl. Radiat. Isot.*, 143, 6-10, 2019.
[38] M. Şekerci, H. Özdoğan, and A. Kaplan, "Charged Particle Penetration Distance and Mass Stopping Power Calculations on Some Nuclear Reactor Control Rod Materials," *Erzincan Üniversitesi Fen Bilimleri Enstitüsü Dergisi*, 12, 1103-1115, 2019.
[39] H. Özdoğan, V. Çapalı, and A. Kaplan, "Reaction cross section stopping power and penetrating distance calculations for the structural fusion material 54Fe in different reactions," *J. Fusion Energy*, 34, 379-385, 2015.
[40] M.I. Sayyed, A. Kumar, H. O Tekin, R. Kaur, M. Singh, O Agar, and M. U. Khandaker, "Evaluation of gamma ray and neutron shielding features of heavy metals doped Bi2O3 BaO Na2O MgO B2O3 glass systems," *Prog. Nucl. Energy*, 118, 103118, 2020.
[41] A. Kumar, D. K. Gaikwad, S. S. Obaid, H. O. Tekin, O. Agar, and M. I. Sayyed, "Experimental studies and Monte Carlo simulations on gamma ray shielding competence of 30 x PbO 10WO3 10Na2O 10MgO 40 x B2O3 glasses," *Prog. Nucl. Energy*, 119, 103047, 2020.
[42] M. I Sayyed, O Agar, A. Kumar, H. O. Tekin, D. K. Gaikwad, and S. S Obaid, "Evaluation of gamma ray and neutron shielding features of heavy metals doped Bi2O3 BaO Na2O MgO B2O3 glass systems," *Chem. Phys*., 529, 110571, 2020.
[43] O. Kilicoglu, E. E. Altunsoy, O. Agar, M. Kamislioglu, M. I. Sayyed, H. O. Tekin, and N. Tarhan, "Synergistic effect of La2O3 on mass stopping power MSP projected range PR and nuclear radiation shielding abilities of silicate glasses," *Results Phys.*, 14, 102424, 2019.
[44] A. Sharma, M. I. Sayyed, O. Agar, and H. O. Tekin, "Simulation of shielding parameters for TeO2 WO3 GeO2 glasses using FLUKA code," *Results Phys.*, 13, 102199, 2019.
[45] M. Bencheikh, A. Maghnouj, and J. Tajmouati, "Photon beam softening coefficient determination with slab thickness in small filed size: Monte Carlo study," *Phys. Part. Nucl. Lett.*, 14, 963-970, 2017.
[46] O. Karaman, H. Özdogan, Y. A. Üncü, C. Karaman, and A. G. Tanır, "Investigation of the effects of different composite materials on neutron contamination caused by medical LINAC," *Kerntechnik*, 85, 401-407, 2020.
[47] A. H. Taqi and H. J. Khalil, "Experimental and theoretical investigation of gamma attenuation of building materials," *J. Phys. G.*, 7, 6-13, 2017.

[48] H. Zhou, P. J. Keall, and E. E. Graves, “A bone composition model for Monte Carlo x-ray transport simulations,” *Med. Phys.*, 36, 1008-1018, 2009.